Current-Voltage Characteristic and Shot Noise of Shift Current Photovoltaics

Takahiro Morimoto,[1] Masao Nakamura,[2,3] Masashi Kawasaki,[2,4] and Naoto Nagaosa[2,4]
[1]Department of Physics, University of California, Berkeley, California 94720, USA
[2]RIKEN Center for Emergent Matter Science (CEMS), Wako, Saitama 351-0198, Japan
[3]PRESTO, Japan Science and Technology Agency (JST), Kawaguchi, Saitama 332-0012, Japan
[4]Department of Applied Physics and Quantum-Phase Electronics Center, University of Tokyo, Bunkyo, Tokyo 113-8656, Japan

(Received 5 July 2018; revised manuscript received 17 October 2018; published 28 December 2018)

We theoretically study the current-voltage relation, the $I-V$ characteristic, of the photovoltaics due to the shift current, i.e., the photocurrent generated *without* the external dc electric field in noncentrosymmetric crystals through the Berry connection of the Bloch wave functions. We find that the $I-V$ characteristic and shot noise are controlled by the difference of group velocities between conduction and valence bands, i.e., $v_{11}-v_{22}$, and the relaxation time τ. Since the shift current itself is independent of these quantities, there are a wide variety of possibilities to design it to maximize the energy conversion rate and also to suppress the noise. We propose that the Landau levels in noncentrosymmetric two-dimensional systems are a promising candidate for energy conversion.

DOI: 10.1103/PhysRevLett.121.267401

Introduction.—There are variety of nonlinear optical processes which are intensively studied especially since strong laser light became available [1,2]. Of particular interest is the generation of dc photocurrent induced by the light excitations aiming at application to solar cells. In the conventional setup, the light is injected to the p-n junction and the photogenerated electrons and holes are separated by the built-in potential gradient. In this situation, the diffusive motion of electrons and holes into the electrode is required to obtain the dc current. On the other hand, the focus of recent intensive attention is the shift current in noncentrosymmetric crystals, which does not require an interface such as the p-n junction [3–8]. In this case, the broken spatial inversion symmetry $\mathcal{I}$ of the crystal structure determines the direction of the photocurrent *without* the external dc electric field. The shift current is regarded as one of the possible microscopic mechanisms of the highly efficient solar cell action in perovskite oxides [9–12]. From the theoretical point of view, shift current originates from the quantum geometric nature of the Bloch wave functions in noncentrosymmetric solids [8,13]. Due to the conjugate relation between the position x and the momentum $p=\hbar k$, x is represented by $i\hbar\partial/\partial p$. ($\hbar$ is the Planck constant divided by 2π.) From this relation applied to the Bloch wave functions of solids, there appears the intracell coordinate x_n for the wave packet made from each Bloch wave function $\langle x|\psi_n(k)\rangle = e^{ikx}\langle x|nk\rangle$ as

$$x_n = a_n(k) = -i\langle nk|\nabla_k|nk\rangle, \tag{1}$$

which is called the Berry connection [14]. The optical transitions between the valence and conduction bands induces the intracell coordinates to shift, which results in the dc current. This is the mechanism of the shift current in noncentrosymmetric crystals. [Note that $a_n(k)$ is 0 for the centrosymmetric crystal with time-reversal symmetry.] The expression for the shift current contains only the interband matrix elements of the current, which is related to the Berry connection defined above, in sharp contrast to the usual photocurrent by the classical motion of carriers described by the intraband matrix elements of the current, i.e, the group velocity. Therefore, it is expected that the physical nature of the shift current is distinct from that of the conventional current.

In Ref. [8], a theoretical framework has been developed to treat the shift current of the two-band model analytically, by combining the Keldysh method and Floquet formalism. The relaxation of electrons $\Gamma=\hbar/\tau$ is introduced, and the competition between the stimulated transitions, i.e., recombining electrons and holes, and the nonradiative relaxation is found to be described by the factor $\Gamma E^2/\sqrt{(eEr)^2+\Gamma^2}$ (r is a constant having a dimension of length). Namely, the nonradiative relaxation Γ, which has no directional dependence, is needed for the finite shift current, while the stimulated transition induces the back flow of the current. This dependence on the strength of the electric field E has been recently observed in SISb by THz spectroscopy [15].

In realistic setup of solar cell action, the voltage at open circuit conditions is often measured, which determines the power conversion rate. Therefore, the $I-V$ characteristics of the shift current is an important issue [Fig. 1(a) and 1(b)]. Another possible application is the photodetector [Fig. 1(c)]. For that purpose, the noise of the shift current needs to be analyzed. In the present Letter, we theoretically study these two issues. The former is achieved by developing a new theoretical technique that combines

the gauge invariant formulation of Keldysh Green's function with the Floquet theory description of shift current [8]. The latter is done by computing correlation functions with nonequilibrium Green's functions on top of Floquet theory approach.

$I-V$ characteristics of shift current photovoltaics.—In the experimental setup to measure shift current, an electrical circuit is formed by attaching two electrodes to the crystal and including resistors as shown in Fig. 1(a). The relationship between the voltage between the two electrodes and the current flowing through the crystal is the fundamental information that is necessary to design the solar cells [Fig. 1(b)]. Especially, the open circuit voltage is an important quantity for the energy conversion rate. The shift current involves the interband transitions that inevitably create the electrons and holes. Therefore, the additional current due to these photogenerated carriers and their interference with the shift current should be analyzed, which we undertake in this section.

We study a system in an external electric field by using gauge invariant formulation of Keldysh Green's function and its gradient expansion. In the presence of an external dc electric field $E_{\rm dc}$, the Green's function is expanded with respect to $E_{\rm dc}$ as $G(E_{\rm dc}) = G_0 + (\hbar e E_{\rm dc}/2) G_E + O(E_{\rm dc}^2)$ [16–18]. In addition, we employ the Floquet two band model to incorporate ac electric field $E_{\rm light}$ of constant light

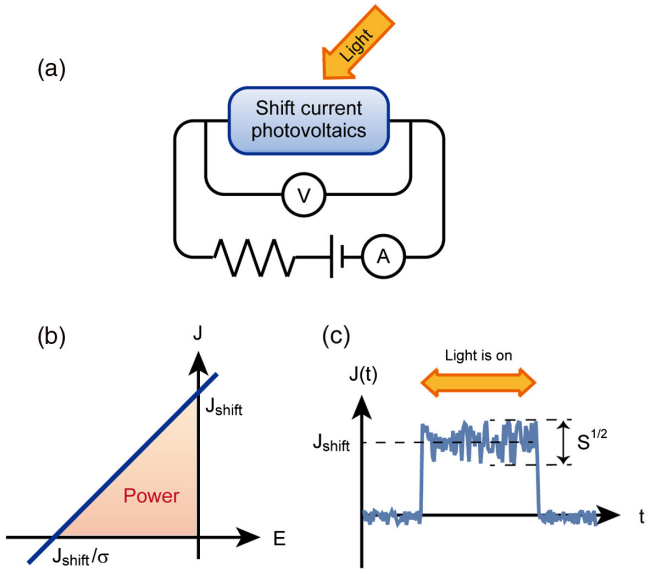

FIG. 1. Schematic picture of $I-V$ characteristics and photodetection in shift current photovoltaics. (a) Setup to measure $I-V$ and photocurrent. (b) $I-V$ characteristics of shift current photovoltaics. In this Letter, we consider current density J as a function of the electric field E. (c) Shot noise in shift current photovoltaics. When the light is off, current fluctuates around zero due to thermal noise which can be neglected in zero temperature. When light is on, shift current flows and additional current fluctuation appears due to photocarriers in the nonequilibrium steady state.

that is irradiated to the sample and produces shift current [8]. We focus on the valence band with one photon and the conduction band with zero photon. The Floquet Hamiltonian is given by

$$H_F = \begin{pmatrix} \epsilon_1 + \hbar\omega & eAv_{12} \\ eAv_{21} & \epsilon_2 \end{pmatrix}, \tag{2}$$

when the static Bloch Hamiltonian H (without the light field) is diagonalized as $H(k)|u_i(k)\rangle = \epsilon_i(k)|u_i(k)\rangle$ with the energy dispersion $\epsilon_i(k)$ and the Bloch wave function $|u_i(k)\rangle$ for the ith band. Here, the velocity matrix element is defined as $v_{ij} = (1/\hbar)\langle u_i|\partial_k H|u_j\rangle$, and $A = E_{\rm light}/\omega$ with the strength $E_{\rm light}$ and the frequency ω of the light electric field. The indices 1 and 2 refer to valence and conduction bands, respectively. For details, see Supplemental Material (SM) [19].

With this setup, the $I-V$ characteristic of shift current materials is given by

$$J(E_{\rm dc}) = J_{\rm shift} + \sigma_E E_{\rm dc}, \tag{3}$$

with

$$J_{\rm shift} = \frac{2\pi e^3}{\hbar^2\omega^2}|E(\omega)|^2 \int [dk] {\rm Im}\left[\left(\frac{\partial v}{\partial k}\right)_{12} v_{21}\right] \delta(\omega_{21}-\omega), \tag{4}$$

$$\sigma_E = \frac{4\pi e^4}{\hbar^3\omega^2}|E(\omega)|^2\tau^2 \int [dk]|v_{12}|^2(v_{11}-v_{22})R'\delta(\omega_{21}-\omega), \tag{5}$$

where $[dk] \equiv dk/(2\pi)^d$ with the dimension d, $R = {\rm Im}[(\partial_k v)_{12}/v_{12}]$, $R' = {\rm Re}[(\partial_k v)_{12}/v_{12}]$, and $\omega_{21} = (\epsilon_2-\epsilon_1)/\hbar$. We note that $R = \partial_k {\rm Im}[\log v_{12}] + a_1 - a_2$ is called shift vector related to the shift of intracell coordinates between the two bands. (For derivation, see SM).

The physical meaning of the above expressions can be understood as follows. In our setup, the sample is subjected to constant light field, which produces the constant shift of the electrons associated with the interband transitions leading to the shift current $J_{\rm shift}$. With the dc electric field, the accelerated motion of the photoexcited electrons and holes generates additional current $\sigma_E E_{\rm dc}$, which is proportional to the difference of the group velocities between the conduction and valence bands, i.e., $v_{11}-v_{22}$. The former, i.e., shift current $J_{\rm shift}$, is basically independent of the lifetime τ of the electrons, while the latter is proportional to τ^2. This is because the photocarrier density is proportional to the recombination time τ and their mobility is also proportional to the scattering time τ. (Note that both recombination and scattering times are described by the same τ in our formalism.) Therefore, it is expected that the shift current $J_{\rm shift}$ (at zero bias) is almost independent of

the disorder and temperature of the sample, while the slope in $I-V$ characteristics that corresponds to the additional current driven by $E_{\rm dc}$ is strongly disorder and temperature dependent through the τ^2 factor.

Current noise in shift current photovoltaics.—The transport current is inevitably associated with the noise. There are two types of the current noise [24,25]. One is the equilibrium noise, i.e., Nyquist noise, which is independent of the details of the system and is given only by the impedance $Z(\omega)$ of the current circuit at frequency ω. The spectrum of the current fluctuation is given by $(J^2)_\omega = [\omega\Re[1/Z(\omega)]\coth(\omega/2T)$. The other is the nonequilibrium noise induced by the current flow. At low temperatures, the quantum mechanical shot noise is the dominant contribution, which originates from the discrete nature of the electron and its charge $-e$. The shot noise is characterized by the Fano factor $F=(J^2)_{\omega=0}/I$ with I being the current. For the ideal situation, $F=2e$ and the shot noise is used as a tool to determine the charge of the carriers.

As mentioned in the introduction, the shift current is distinct from the conventional current in that shift current is intimately related to the wave nature of the electrons that is characterized by the off-diagonal matrix elements of the current operator. Therefore, it is expected that the noise of the shift current is distinct from that of the conventional one.

Motivated by this consideration, we study current noise in shift current photovoltaics. We compute autocorrelation of local current operator $v_{\rm loc}$ defined at one point (e.g., $x=0$) in the bulk, which is given by $v=(1/2L)\sum_{k,k'}(v_k+v_{k'})c_k^\dagger c_{k'}$, where L is the sample size, and k and k' satisfy $|k-k'|<1/l$ with the size of the electrode l [26]. The current noise is given by the zero frequency component of the autocorrelation as

$$S=\int dt(\langle v_{\rm loc}(t)v_{\rm loc}(0)\rangle-\langle v_{\rm loc}\rangle^2). \tag{6}$$

To describe the nonequilibrium steady state under light irradiation that supports shift current, we again use the Floquet two band model H_F. By using Green's functions in the Floquet two band model derived in the SM, the noise S can be expressed as

$$S=\frac{e^4}{\hbar^2\omega^2}E^2\tau\int[dk]|v_{11}-v_{22}||v_{12}|^2\delta(\omega_{21}-\omega). \tag{7}$$

(For derivation, see SM.) This expression shows that the noise is proportional to the relaxation time τ and may be interpreted as temperature noise in the steady state with the effective temperature proportional to the transition rate $\approx|v_{12}|^2$. Interestingly, the noise S does not have a part that corresponds to usual current noise in the equilibrium systems which is proportional to the current ($S\propto J$). This means that the noise S is substantially suppressed if the relaxation time τ is very short or two bands are parallel with each other ($v_{11}-v_{22}\approx 0$), In such cases, shift current photovoltaics can show much less noise than conventional metals subject to current noise.

Shift current in Landau levels.—In the previous sections, we have shown that both the $I-V$ characteristics and the noise are governed by the difference of group velocities of conduction and valence bands, i.e., $v_{11}-v_{22}$, and the relaxation time τ. In particular, when $v_{11}-v_{22}=0$, the current is independent of the voltage and also the noise is 0. This is an ideal situation both for the solar cells and photodetectors. However, it is usually difficult to realize the situation of "parallel" dispersion between the conduction and valence bands. Here we propose the dispersonless Landau levels in 2D offers a promising laboratory to test the ideal developed above. The dc current in the flat band system can be also a smoking gun experiment for the unconventional nature of the shift current distinct from the usual photocurrent by the diffusive motion of photocarriers. More explicitly, we consider the two systems, i.e., the Landau levels of graphene and Landau levels of the surface state of three dimensional topological insulator.

We first study shift current in graphene Landau levels (LLs). Since LLs have flat band dispersion, we expect that the current noise is suppressed and the power of shift current is enhanced in LLs. In order to take into account the effect of inversion breaking in graphene, we consider Dirac Hamiltonian with a trigonal warping term [27–29],

$$H=v_F\begin{pmatrix}0 & \pi^\dagger\\ \pi & 0\end{pmatrix}+\eta\kappa\begin{pmatrix}0 & \pi^2\\ (\pi^\dagger)^2 & 0\end{pmatrix}, \tag{8}$$

with Fermi velocity v_F, strength of trigonal warping κ, $\pi=k_x\pm ik_y$, and $\eta=\pm1$ for K and K' valleys, respectively. In the presence of magnetic field, the momentum operators are written as $\pi=(\sqrt{2}\hbar/\ell)a^\dagger$ at K and $\pi=(\sqrt{2}\hbar/\ell)a$ and K' with annihilation and creation operators a and $a^\dagger$, and the magnetic length $\ell=\sqrt{\hbar/eB}$. Now let us consider shift current supported by the graphene LLs. We suppose that the Fermi level is located between $n=0$ and $n=1$ LLs, and the sample is irradiated with linearly polarized light along the x direction with the photon energy close to $\hbar\omega_c$. In this case, the photoexcitation takes place from $n=0$ LL to $n=1$ LL. The shift current response $J_y=\sigma_{yxx}|E_x(\omega)|^2$ is given by

$$\sigma_{yxx}(\omega)=\eta\frac{e^3}{\hbar\omega^2\ell^2}v_F\kappa\delta(\omega-\omega_{10}), \tag{9}$$

where $\omega_{10}=(1/\hbar)(\epsilon_1-\epsilon_0)$ with ϵ_0 (ϵ_1) being the energy of $n=0$ ($n=1$) LL. This means that the shift current response vanishes when the optical transition $0\to1$ takes place both at K and K' valleys. This is natural since the

original Hamiltonian has inversion symmetry $\mathcal{I} = \sigma_x \tau_x$, where σ and τ are Pauli matrices acting on sublattice and valley degrees of freedom; nonzero shift current requires the breaking of inversion symmetry. One way to achieve this is introducing staggered potential $m\sigma_z\tau_0$. For example, this situation is realized in graphenes on the substrate of BN, and also in transition metal dichalcogenide (TMDC) such as MoS_2. Staggered potential only shifts the energy of $n = 0$ LL to $-\eta m$ without changing energies of other LLs. Also, it does not change the wave functions of LLs. For example, when the Fermi energy lies between $n = 0$ LLs and $n = 1$ LLs (both at K and K' points) as illustrated in Fig. 2(a), nonzero shift current flows by tuning the photon frequency to either $\hbar\omega_c - m$ (resonant at K valley) or $\hbar\omega_c + m$ (resonant at K') valley.

Next, we move on to shift current in LLs on the surface of topological insulators (TIs). The Hamiltonian is written as [30]

$$H = v_F(p_x\sigma_y - p_y\sigma_x) + \frac{\lambda}{2}(p_+^3 + p_-^3)\sigma_z, \qquad (10)$$

where v_F is the Fermi velocity, λ is the strength of trigonal warping effect, and $p_\pm = p_x \pm ip_y$. The Hamiltonian has C_3 rotation symmetry and reflection symmetry along the x direction $[(k_x, k_y) \to (-k_x, k_y)]$ with $R_x = i\sigma_x$. With C_{3v} symmetry, nonzero components of second order nonlinear conductivity are $\sigma_{yyy} = -\sigma_{yxx}$. The Hamiltonian in the magnetic field is again obtained by replacing the momentum operators with creation or annihilation operators (for details, see SM). The nonlinear conductivity σ_{yyy} in the lowest order in the trigonal warping is given by

$$\sigma_{yyy}(\omega) = -\frac{3e^3}{\sqrt{2}\omega^2\ell^3} v_F\lambda\delta(\omega - \omega_{10}), \qquad (11)$$

when the Fermi energy is located between $n = 0$ and $n = 1$ LLs, and the photon frequency is close to the cyclotron energy ($\omega \sim \omega_c$). [31] A general expression for σ_{yyy} can be found in the SM, and it shows that the two interband transitions $-n \to n + 1$ and $-n - 1 \to n$ (which have the same resonance frequency) make opposite contributions to shift current [see Fig. 2(b)]. In Fig. 2(c), optical absorption shows consecutive peaks from interband contributions while shift current shows only one peak at the resonance $0 \to 1$.

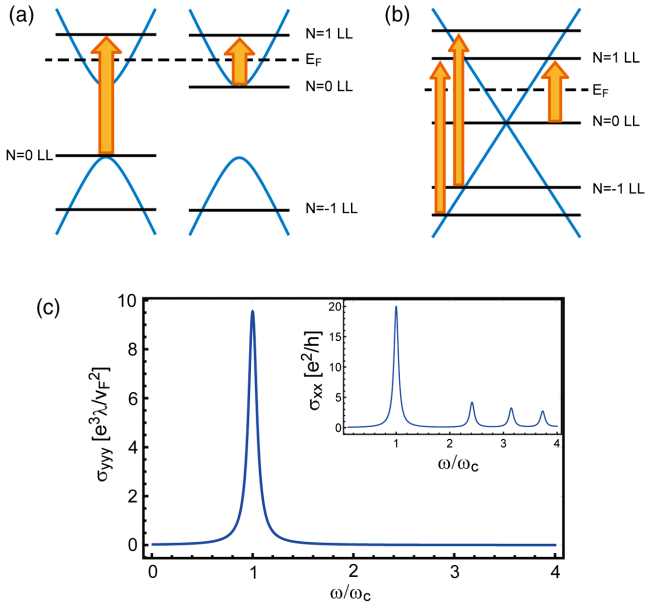

FIG. 2. Optical transitions in LLs in inversion broken 2D systems realized in (a) graphene with staggered potential, and (b) TI surface states. (c) Shift current in TI surface states. We plot the nonlinear conductivity σ_{yyy} as a function of frequency. The inset is for linear conductivity $\sigma_{yy}(\omega)$. Relaxation time is set to $1/\tau = 0.05\omega_c$.

We can estimate photocurrent supported by the LLs as follows. For $B = 1$ T, the cyclotron energy is given by $\hbar\omega = 38$ meV (graphene [27–29]), 22 meV (MoS_2 [32]) and $\hbar\omega = 14$ meV (TI [30]) using material parameters from the references, which falls into a terahertz regime. For the typical relaxation time of $\tau = 1$ ps, the 2D nonlinear conductivity are estimated as $\sigma = 7.3 \times 10^{-12}$ A m/V^2 (graphene), 5.5×10^{-12} A m/V^2 (MoS_2), and 1.7×10^{-11} A m/V^2 (TI). These values exceed σ for a typical 2D shift current material monolayer GeS $\sigma \sim 10^{-14}$ A m/V^2 [33]. We can estimate photocurrent J generated by light intensity I from the formula $J = \kappa I$ with $\kappa = 2\sigma/c\epsilon_0$ [7]. This allows us to convert $\sigma = 1.0 \times 10^{-11}$ A m/V^2 to $\kappa = 7.6 \times 10^{-5}$ (A/m)/(W/cm^2). For example, when a TI of sample size 1 mm is irradiated with $I = 1$ W/cm^2 under $B = 1$ T, the shift current from LLs reaches 100 nA, which is much larger than a photocurrent of 10–100 pA that has been observed for a TI thin film [34].

Finally, we discuss the efficiency of shift current of the LLs. While σ_E becomes zero due to the flat band nature of the LLs, there exists a maximum electric field $E_{\max}$ that we can apply to LL photovoltaics as illustrated in Fig. 3. In the electric field $E_{\rm dc}$, the real space shift of an electron quantified by shift vector R causes energy shift of $eE_{\rm dc}R$. In order that the photoexcitation still takes place in the presence of $E_{\rm dc}$, this energy shift $eE_{\rm dc}R$ should not exceed the band width W of valence and conduction bands [see Fig. 3(c)]. Therefore, the maximum electric field is determined by $E_{\max} = W/eR$. In the case of LLs, the bandwidth is given by $W \simeq \hbar/\tau$ with relaxation time τ. (Here we assume that the sample is irradiated with monochromatic light of cyclotron frequency and the LLs have uniform level broadening of W, where optical transition equally takes place as far as $|E_{\rm dc}| < E_{\max}$.) Now we estimate the monochromatic power conversion efficiency $r = P_{\rm out}/P_{\rm in}$ for monochromatic light with the cyclotron frequency. Here, $P_{\rm out}$ is the power generated by shift

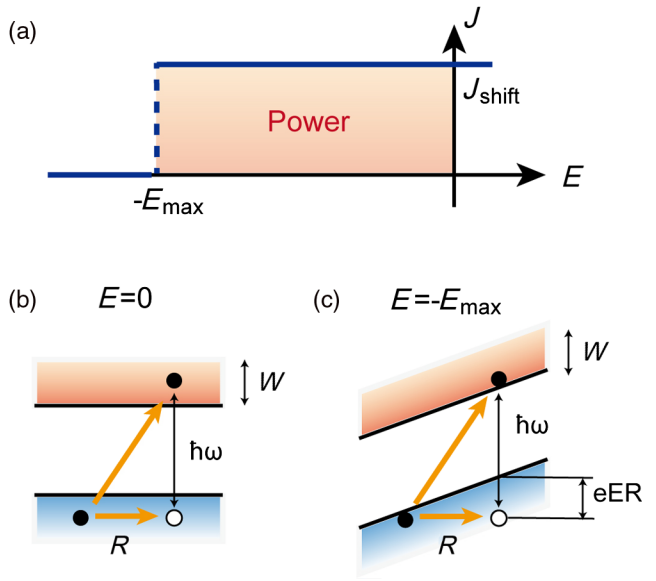

FIG. 3. (a) $I-V$ characteristic of flat band systems. (b) Photoexcitation in zero electric field. (c) Photoexcitation in $E=-E_{\max}$. Real space shift R causes energy shift of eER.

current photovoltaics, which is given by $P_{\rm out}=J_{\rm shift}E_{\max}$, and $P_{\rm in}$ is the power absorbed by the sample that is given by $P_{\rm in}=\sigma^{(1)}(\omega)|E(\omega)|^2$ where $\sigma^{(1)}(\omega)$ is the linear conductivity quantifying the absorption rate of the monochromatic light. By using a rough approximation for Eq. (4) as $J_{\rm shift}\simeq(e/\hbar\omega)|E(\omega)|^2\sigma^{(1)}R$, we obtain the conversion efficiency for flat band systems as

$$r\simeq\frac{W}{\hbar\omega}\simeq\frac{1}{\omega\tau}. \tag{12}$$

For $B=1$ T, the efficiency r becomes as high as $r=11\%$ (graphene), 18% (MoS_2), and 29% (TI) with a typical level broadening $W=4$ meV from impurity scattering.

Discussions.—We have studied $I-V$ characteristics and shot noise in shift current photovoltaics. The derived formulae for them indicate that the slope in the $I-V$ characteristic and the shot noise are strongly disorder and temperature dependent through their τ dependence, while zero bias shift current is independent of disorder and temperature. The formulae also show that it is possible to suppress both the slope in $I-V$ characteristics and the nonequilibrium noise simultaneously by reducing the band widths.

Flat band systems are the ideal laboratory to realize this situation. We have proposed that the LLs of graphene and surface states of 3D TIs are promising candidates for this purpose. We predict that the shift current of LLs is observable with essentially no current fluctuation and with high monochromatic power conversion efficiency. This will offer the sharpest experimental test of the geometrical nature of the shift current. For application as photodetectors for weak intensity light, we also need to consider noise that comes from quantum statistics of photons, which is left for future studies.

We thank J. Orenstein, and J. E. Moore for fruitful discussions. T. M. was supported by the Gordon and Betty Moore Foundation's EPiQS Initiative Theory Center Grant to UC Berkeley, and the Quantum Materials program at LBNL funded by the US Department of Energy under Contract No. DE-AC02-05CH11231. M. N. was supported by PRESTO, JST (No. JPMJPR16R5). M. K. and N. N. were supported by CREST, JST (No. JPMJCR16F1). N. N. was supported by JSPS KAKENHI (No. 18H03676), and ImPACT Program of Council for Science, Technology and Innovation (Cabinet office, Government of Japan, 888176).

[1] N. Bloembergen, *Nonlinear Optics* (World Scientific, Singapore, 1996).
[2] R. W. Boyd, *Nonlinear Optics* (Academic Press, London, 2003).
[3] R. von Baltz and W. Kraut, Phys. Rev. B **23**, 5590 (1981).
[4] J. E. Sipe and A. I. Shkrebtii, Phys. Rev. B **61**, 5337 (2000).
[5] S. M. Young and A. M. Rappe, Phys. Rev. Lett. **109**, 116601 (2012).
[6] S. M. Young, F. Zheng, and A. M. Rappe, Phys. Rev. Lett. **109**, 236601 (2012).
[7] A. M. Cook, B. M. Fregoso, F. De Juan, S. Coh, and J. E. Moore, Nat. Commun. **8**, 14176 (2017).
[8] T. Morimoto and N. Nagaosa, Sci. Adv. **2**, e1501524 (2016).
[9] W. Nie, H. Tsai, R. Asadpour, J.-C. Blancon, A. J. Neukirch, G. Gupta, J. J. Crochet, M. Chhowalla, S. Tretiak, M. A. Alam, H.-L. Wang, and A. D. Mohite, Science **347**, 522 (2015).
[10] D. Shi, V. Adinolfi, R. Comin, M. Yuan, E. Alarousu, A. Buin, Y. Chen, S. Hoogland, A. Rothenberger, K. Katsiev, Y. Losovyj, X. Zhang, P. A. Dowben, O. F. Mohammed, E. H. Sargent, and O. M. Bakr, Science **347**, 519 (2015).
[11] D. W. de Quilettes, S. M. Vorpahl, S. D. Stranks, H. Nagaoka, G. E. Eperon, M. E. Ziffer, H. J. Snaith, and D. S. Ginger, Science **348**, 683 (2015).
[12] A. Bhatnagar, A. R. Chaudhuri, Y. H. Kim, D. Hesse, and M. Alexe, Nat. Commun. **4**, 2835 (2013).
[13] N. Nagaosa and T. Morimoto, Adv. Mater. **29**, 1603345 (2017).
[14] R. Resta, Rev. Mod. Phys. **66**, 899 (1994).
[15] M. Sotome, M. Nakamura, J. Fujioka, M. Ogino, Y. Kaneko, T. Morimoto, Y. Zhang, M. Kawasaki, N. Nagaosa, Y. Tokura, and N. Ogawa, arXiv:1801.10297.
[16] S. Onoda, N. Sugimoto, and N. Nagaosa, Prog. Theor. Phys. **116**, 61 (2006).
[17] N. Sugimoto, S. Onoda, and N. Nagaosa, Phys. Rev. B **78**, 155104 (2008).
[18] T. Morimoto and N. Nagaosa, Sci. Rep. **8**, 2973 (2018).
[19] See Supplemental Material at http://link.aps.org/supplemental/10.1103/PhysRevLett.121.267401 for a Floquet two band model, the gauge invariant formulation of

Keldysh Green's function, and details of the calculations, which includes Refs. [20–23].
[20] J. Rammer and H. Smith, Rev. Mod. Phys. **58**, 323 (1986).
[21] A.-P. Jauho, N. S. Wingreen, and Y. Meir, Phys. Rev. B **50**, 5528 (1994).
[22] H. Aoki, N. Tsuji, M. Eckstein, M. Kollar, T. Oka, and P. Werner, Rev. Mod. Phys. **86**, 779 (2014).
[23] P. J. Sturman and V. M. Fridkin, *Photovoltaic and Photorefractive Effects in Noncentrosymmetric Materials* (CRC Press, Philadelphia, 1992), Vol. 8.
[24] Y. Imry, *Introduction to Mesoscopic Physics*, Mesoscopic Physics and Nanotechnology (Oxford University Press, Oxford, 2002).
[25] E. Lifshitz and L. Pitaevskii, *Statistical Physics, Part 2: Volume 9* (Butterworth-Heinemann, Oxford, 1980), Vol. 9.
[26] D. van der Marel, in *Strongly Correlated Systems* (Springer, Berlin, 2015), pp. 269–296.
[27] T. Ando, T. Nakanishi, and R. Saito, J. Phys. Soc. Jpn. **67**, 2857 (1998).
[28] M. Koshino and E. McCann, Phys. Rev. B **80**, 165409 (2009).
[29] E. McCann and M. Koshino, Rep. Prog. Phys. **76**, 056503 (2013).
[30] L. Fu, Phys. Rev. Lett. **103**, 266801 (2009).
[31] We note that the nonlinear conductivity in TI surface states show a different B dependence ($\propto B^{3/2}$ from $\ell \propto 1/\sqrt{B}$) compared to graphene ($\propto B$). This is a consequence of different forms of trigonal warping ($\propto p^3$ in TI and $\propto p^2$ in graphene).
[32] A. Kormányos, V. Zólyomi, N. D. Drummond, P. Rakyta, G. Burkard, and V. I. Fal'ko, Phys. Rev. B **88**, 045416 (2013).
[33] T. Rangel, B. M. Fregoso, B. S. Mendoza, T. Morimoto, J. E. Moore, and J. B. Neaton, Phys. Rev. Lett. **119**, 067402 (2017).
[34] K. N. Okada, N. Ogawa, R. Yoshimi, A. Tsukazaki, K. S. Takahashi, M. Kawasaki, and Y. Tokura, Phys. Rev. B **93**, 081403 (2016).